X-ray Analysis of Structural Changes Induced by Reduced Nicotinamide Adenine Dinucleotide When Bound to Cysteine-46-Carboxymethylated Liver Alcohol Dehydrogenase†

Eila S. Cedergren-Zeppezauer* and Inger Andersson

Department of Molecular Biology, Swedish University of Agricultural Sciences, Uppsala Biomedical Center, S-751 24 Uppsala, Sweden

Simone Ottonello and Enrico Bignetti

Institute of Molecular Biology, University of Parma, Cornocchio, I-43100 Parma, Italy

Received October 18, 1984; Revised Manuscript Received February 5, 1985

ABSTRACT: The structure of the complex between Cys-46-carboxymethylated horse liver alcohol dehydrogenase (CM-LADH) and reduced nicotinamide adenine dinucleotide (NADH) has been determined by X-ray analysis. The complex represents NADH binding to the orthorhombic, "open" conformation of the enzyme. Coenzyme binding here induces a local structural change in the peptide loop 293–297, but there is no domain rotation, as observed for the "closed" conformation of the protein. This local movement of a few residues in the loop is sufficient to trap the nicotinamide ring of NADH within the active-site area close to a productive binding position. The carboxymethyl group on the zinc ligand cysteine-46 is oriented between the pyrophosphate bridge of NADH and the guanidinium group of arginine-369 and can occupy this position because the coenzyme binding cleft remains open and unchanged upon coenzyme binding. The zinc coordination sphere is distorted, and the position of the metal atom is shifted 1 Å compared to native unliganded LADH. The distance between the zinc ion and the sulfur of the alkylated cysteine residue is of the order of 3 Å. Alkylation experiments were performed at 0.15 and 10 mM iodoacetate, and peptide maps were examined. Gentle treatment with reagent yields an enzyme product which is substituted at only one of the two zinc binding sites per subunit of LADH (Cys-46). This enzyme species maintains its structural integrity; it binds coenzyme which induces conformational changes resolved into two steps. Thus, in addition to the orthorhombic complex, a crystalline NADH complex in the closed conformation of CM-LADH was obtained. These crystals showed enzymic activity, and single crystals were analyzed with microspectrophotometric methods. Formation of the stable crystalline abortive complex between CM-LADH–NAD^+ and 4-*trans*-(*N*,*N*-dimethylamino)cinnamaldehyde (DACA) could be observed upon addition of excess aldehyde to the closed complex of CM-LADH–NADH. The CM-LADH–NAD^+–DACA complex is characterized by an intense absorption band with a λ_{max} at 456 nm which corresponds to a shift in the spectrum of free DACA of approximately 60 nm. At the higher concentration of iodoacetate, three of the cysteine ligands to the second zinc atom (Cys-100, -103, and -111) are alkylated in addition to Cys-46. This enzyme product rapidly denatures and cannot be crystallized under our conditions. This is an experimental indication that the intact noncatalytic zinc binding site contributes to the structural stability of the protein.

Cysteine-46-carboxymethylated liver alcohol dehydrogenase (CM-LADH)[1] is an active enzyme species (Reynolds & McKinley-McKee, 1975; Hardman, 1976) even though the catalytic activity is greatly inhibited compared to unsubstituted LADH when ethanol is used as a substrate at neutral pH. However, at high pH, CM-LADH is more active than the native enzyme when aldehyde substrates are converted (Reynolds & McKinley-McKee, 1975; Dahl & Dunn, 1984b). The introduction of a carboxymethyl group on one of the cysteine ligands to the active-site zinc atom (Zeppezauer et al., 1975) causes changes in some of the kinetic properties of the enzyme. The rate of hydride transfer is 700-fold lower for CM-LADH (Hardman, 1976) and is the rate-limiting step for alcohol oxidation. This is in contrast to native LADH for which the dissociation rate of NADH from the enzyme limits the turnover number (Shore & Gutfreund, 1970; Kamlay & Shore, 1983). In a recent study of the reduction of the aldehydes 4-*trans*-(*N*,*N*-dimethylamino)cinnamaldehyde (DACA) and *p*-nitrobenzaldehyde, it was found that also for this reaction the rate-limiting step involves hydride transfer (Dahl & Dunn, 1984b).

CM-LADH shows basic differences in the ability to form ternary complexes (Reynolds & McKinley-McKee, 1975; Dahl & Dunn, 1984b) compared to the unlabeled enzyme. Furthermore, there is no detectable formation of a binary complex with NADH at pH 10. The binding strength for NAD^+ does not increase to a maximal value at high pH in CM-LADH

† This work was supported by Grant 2767 from the Swedish Natural Science Research Council, by Grant 13X-3532 from the Medical Research Council, and by the Consiglio Nazionale delle Ricerche, Italy.

[1] Abbreviations: F_{obsd}, observed structure factor; F_{calcd}, calculated structure factor; Tris, tris(hydroxymethyl)aminomethane; MPD, 2-methyl-2,4-pentanediol; DACA, 4-*trans*-(*N*,*N*-dimethylamino)cinnamaldehyde; PEG, poly(ethylene glycol); LADH, horse liver alcohol dehydrogenase (EC 1.1.1.1); CM-LADH, Cys-46-carboxymethylated horse liver alcohol dehydrogenase; trypsin, EC 3.4.21.4, L-1-(tosylamido)-2-phenylethyl chloromethyl ketone treated; EDTA, ethylenediaminetetraacetic acid; Tes, *N*-[tris(hydroxymethyl)methyl]-2-aminoethanesulfonic acid.

0006-2960/85/0424-4000$01.50/0

in contrast to what is found for the native enzyme (Theorell & McKinley-McKee, 1961; Dalziel, 1963; Taniguchi et al., 1967).

Reactions which are pH dependent also differ. The group on the enzyme which has an apparent pK_a value of 9.6 is not affected by the carboxymethylation of cysteine-46, but the perturbation of this pK_a value down to 7.6, which is described for the native enzyme, is not observed upon binding of NAD^+ to CM-LADH (Parker et al., 1978; Khalifah & Sutherland, 1979). The decay of the intermediate formed when the native enzyme is mixed with NADH and the DACA substrate is dependent on a group with an apparent pK_a of 6 (Morris et al., 1980) whereas the same process is virtually pH independent for CM-LADH (Dahl & Dunn, 1984b). Many of the changed properties of CM-LADH have been attributed to the altered charge distribution at the active-site zinc center.

The single substitution of cysteine-46 with iodoacetate in the crystalline state was utilized as a spacial marker to confirm the position of this residue (Zeppezauer et al., 1975) after the structure determination of the "open conformation" of LADH (Eklund et al., 1976). In this coenzyme-free structure, the carboxymethyl group is oriented so that it does not block the coenzyme binding cleft or the substrate binding site. Minor changes in the protein structure involving an interior arginine side chain in contact with the label could be observed at low resolution. No determination of the bond length between the zinc atom and the thioether sulfur could be made.

A brief review of the structure of native LADH and its complexes with coenzyme, coenzyme analogues, inhibitors, and substrates has recently appeared (Eklund & Brändén, 1983). It is well established that the triclinic space group and the monoclinic space group $P2_1$ both occur only when the protein is in the "closed" conformation (Eklund et al., 1981; Samama, 1979; Schneider, 1983). In this conformation, the A-stereospecific side of the nicotinamide ring of NADH faces the active-site zinc and the substrate binding cleft. Domain rotatations (Eklund et al., 1984) in the bilobal subunit have enclosed the ring at an interior region of the active-site area, and therefore, the ring orientation becomes restricted due to spatial limitations.

Structure analyses of coenzyme complexes in the open or the closed conformation of LADH (Samama et al., 1977, 1981; Eklund et al., 1981, 1982a,b; Cedergren-Zeepezauer et al., 1982; Cedergren-Zeppezauer, 1983; Schneider et al., 1983) have demonstrated that the conformational transition is a process which can be influenced by the nature of the fourth ligand to the active-site zinc ion or by substitutions in the coenzyme molecule. It was therefore of interest to examine how the presence of the carboxymethyl group in the active-site zinc environment would affect the protein–NADH interactions, since we observed that a crystalline CM-LADH–NADH complex could be formed in which the protein is maintained in the open conformation. We present here the X-ray structure analysis of this complex, as well as microspectrophotometric studies of the NADH complex in the closed conformation. Furthermore, we identify, in the primary structure, the differences in cysteine residues that become labeled at low concentrations of iodoacetate—used to prepare crystalline complexes of CM-LADH in this work—and at higher concentrations of reagent frequently used in experiments with CM-LADH in solution (Reynolds & McKinley-McKee, 1975; Hardman, 1976; McFarland et al., 1977; Parker et al., 1978).

Materials and Methods

Microcrystalline horse liver alcohol dehydrogenase was obtained from Boehringer Mannheim GmbH (Mannheim, FRG) and crystallized as described before (Zeppezauer et al., 1975). Trypsin, used for digestion experiments, was obtained from Worthington Biochemical Corp. NADH was purchased from Sigma (St. Louis, MO), high-purity buffer salts were from Serva (Heidelberg, FRG), and suprapure chemicals were from Merck. Iodoacetic acid (Merck) was recrystallized in heptane; iodo[2-^{14}C]acetic acid was obtained from the Radiochemical Center (Amersham, England). 2-Methyl-2,4-pentanediol (MPD) (Eastman Kodak Co.) was doubly distilled under purified nitrogen in the presence of borohydride. 4-*trans*-(*N*,*N*-Dimethylamino)cinnamaldehyde (DACA) (Aldrich) was sublimated prior to use. Other enzyme substrates were used without further purification. Sephadex G25 was obtained from Pharmacia (Uppsala, Sweden). Great care was taken to avoid heavy-metal contamination.

Samples Used for X-ray Analysis. Conditions for providing complete carboxymethylation of Cys-46 without nonspecific modification on the other 13 cysteine residues per subunit of crystalline dimeric LADH have been determined previously (Zeppezauer et al., 1975). Iodoacetate (3.3 μmol) was added by dialysis to 0.25 μmol of subunit at pH 7.8 in 0.05 M Tris-HCl, without the addition of imidazole. Although imidazole enhances the rate of incorporation of the carboxymethyl group on Cys-46 (Evans & Rabin, 1968; Reynolds & McKinley-McKee, 1969; Reynolds et al., 1970; Dahl & McKinley-McKee, 1981; Syvertsen & McKinley-McKee, 1983), we have avoided it for two reasons: (1) Imidazole is tightly bound to the labeled protein and is not separated from the binding site by gel filtration (Jones & Khalifah, 1980). (2) Zinc-bound imidazole is an inhibitor for the coenzyme-induced conformational change in native LADH (Cedergren-Zeppezauer, 1983). After 24 h at 4 °C, the reaction mixture was passed through a small Sephadex G25 column, equilibrated with 0.1 M Tris-HCl, pH 8.4. The enzymic activity toward ethanol was measured over the whole protein peak and was found to be less than 5% compared to native enzyme (Reynolds & McKinley-McKee, 1969). Fractions containing 0.7–0.85% protein/mL were pooled and dialyzed against 0.05 M Tris-HCl, pH 8.4, and used for crystallization to obtain X-ray-grade crystals. The complex between CM-LADH and NADH (0.5 mM) was formed in solution. By small additions of MPD over a period of a few weeks, large orthorhombic crystals, of the space group $C222_1$, were formed (final solvent concentration 25% v/v). The zinc content of dissolved CM-LADH crystals was determined on a Perkin-Elmer 400 atomic absorption spectrophotometer and was found to be 1.8–2.0 mol/subunit, similar to native enzyme samples.

Five crystals (cell dimensions: $a = 56.0 \pm 0.1$ Å, $b = 75.2 \pm 0.1$ Å, $c = 181.7 \pm 0.2$ Å) were used to collect 5970 reflections to 3.2-Å resolution on a Stoe four-circle diffractometer. The procedures for data collection and data reduction have been described earlier (Eklund et al., 1976, 1981). The crystals were sensitive to X-ray damage, and high-resolution data have been difficult to obtain. The time-dependent decrease in intensity due to radiation damage was not allowed to exceed 15%. In addition to the 30 standard reflections routinely measured for each crystal at the start of data collection, 50 overlapping reflections between crystals were used to calculate R values ($|F_1| - |F_2|/|F_1|$) between individual crystals. R values ranged between 3.5% and 4%. The observed structure factors were combined with calculated phase angles derived from the crystallographic refinement of the native, orthorhombic model (T. A. Jones and H. Eklund, unpublished results). The interpretation of difference Fourier maps with amplitudes $||F_{obsd}| - |F_{calcd}|$ or $|2|F_{obsd}| - |F_{calcd}||$ was made in

an interactive graphics display system (VG 3404) using the FRODO program (Jones, 1982). The strategy for the model-building procedure has been extensively described elsehwere (Cedergren-Zeppezauer et al., 1982). Structure factors and Fourier maps were calculated by using the PROTEIN program of W. Steigemann. The crystallographic refinement of the CM-LADH–NADH complex was made by using the programs COREL5 (Sussman et al., 1977) and EREF (Jack & Levitt, 1978). Stereo diagrams were plotted on a Hewlett-Packard plotter in conjunction with the VG 3404 graphics system by using computer programs written by T. A. Jones. Space group determinations on different crystal forms were made from precession photographs.

Samples Used for Peptide Analysis. Two samples were compared. (1) Twenty milligrams of crystalline LADH was dissolved in 1.5 mL of 0.1 M phosphate buffer, pH 7, containing 0.1 M KCl. The enzyme was first dialyzed against phosphate buffer, pH 7.9, and finally against 5 mM imidazole buffer, pH 7.8. A solution of iodo[2-^{14}C]acetate (50 μL; 0.5 mCi/mL) was added to the sample to give a final iodoacetate concentration of 10 mM. After 1.5 h, the sample was applied to a Sephadex G25 column. The protein peak was pooled, and the enzyme was extensively dialyzed against doubly distilled water. The concentration of radioactive iodoacetate used in this sample corresponds to the highest concentration range used in kinetic experiments with Cys-46-labeled LADH (Reynolds & McKinley-McKee, 1975; Hardman, 1976; Parker et al., 1978). Samples treated with 10 mM iodoacetate could not be crystallized, neither in the presence nor in the absence of NADH. Rapid denaturation of the protein was observed. (2) Ten milligrams of recrystallized LADH was carboxymethylated according to the dialysis method of Zeppezauer et al. (1975). Iodo[2-^{14}C]acetate (0.5 mCi/mL) was added to an outer solution to give a final iodoacetate concentration of 0.15 mM. The labeled crystals were dissolved and dialyzed against doubly distilled water. The concentration of radioactive iodoacetate used in this sample corresponds to the concentration of reagent used in order to obtain crystalline CM-LADH–NADH complexes.

The two samples were then fully carboxymethylated with nonradioactive iodoacetate, in guanidine hydrochloride, in order to achieve chemically homogeneous proteins differing only in their isotope content. The proteins were reduced (37 °C, 2 h) with dithioerythritol (0.5 μmol/mg of protein) in 6 M guanidine hydrochloride, 2 mM EDTA, and 0.1 M Tris, pH 8.1 (10 mg of protein/mL) of solution), 1.6 μmol of iodoacetate/mg of protein was added (37 °C, 2 h), and the excess reagent was removed by dialysis against 1 mM HCl. The fully carboxymethylated samples were digested with trypsin (37 °C, 4 h) at an enzyme to CM-LADH weight ratio of 1:100, in 0.1 M ammonium bicarbonate. The digests were subjected to thin-layer electrophoresis and chromatography under conditions described earlier (Carlsson et al., 1976). The peptide maps were revealed by autoradiography and finally stained with ninhydrin.

Samples Used for Microspectrophotometric Measurements on Single Crystals. UV–visible absorption spectra on single crystals were recorded on an automatic Zeiss microspectrophotometer operating over the wavelength interval 240–1200 nm. The microscope stage was connected to a cryostat, and measurements were performed at 10 °C. Data acquisition and evaluation of spectra were controlled by the program λ-SCAN. Details about the handling of LADH crystals for spectral recording and determination of enzyme activity have been described earlier (Bignetti et al., 1979). The spectra presented in this work were measured with unpolarized light.

The crystalline material prepared for microspectrophotometric measurements was carboxymethylated according to Zeppezauer et al. (1975). CM-LADH–NADH crystals precipitated with MPD as described above were thin (0.1–0.05 mm) orthorhombic plates suitable in size for mounting between quartz object glasses. Spectra of crystals of the complex between native LADH, NADH, and dimethyl sulfoxide, precipitated with MPD according to the procedures described by Eklund et al. (1981), were also recorded. The enzymic activity of dissolved carboxymethylated crystals was 4% of that of native enzyme toward ethanol as substrate. The K_m value for 1-butanol was determined to be 0.37 mM in agreement with the value reported by Reynolds & McKinley-McKee (1975).

The crystals of the orthorhombic CM-LADH–NADH complex precipitated with MPD were tested in the following way: (1) λ_{max} was determined for enzyme-bound NADH. Estimation of the concentration of bound coenzyme (Bignetti et al., 1979) correlated with the determination of the protein concentration of the dissolved crystals after the recording of single-crystal spectra (the Bio-Rad assay was used). (2) They were tested for enzymic activity in single crystals using benzaldehyde and DACA as the substrates. (3) They were recrystallized with poly(ethylene glycol) (PEG). The orthorhombic CM-LADH–NADH crystals were dissolved in 0.1 M phosphate buffer (pH 7.5)/0.5 mM NADH and extensively dialyzed to remove the recipitant MPD.

Crystallization of CM-LADH–NADH complexes in PEG, from a solution prepared according to (3) or from freshly carboxymethylated microcrystalline LADH suspensions, was achieved in the following way: A sealed siliconated glass petri dish was used as the crystallization vessel for vapor diffusion experiments. Twenty-five to thirty microliters of large droplets was prepared containing 10 μg/μL CM-LADH, 0.5–1 mM NADH, and 1.5–2% PEG 10 000 at pH 7.8 in 0.05 M Tes/NH_3 (or OH^-). Eight to ten droplets per petri dish were equilibrated against a reservoir solution containing 4–7 mL of a mixture of buffer and 5–9% PEG 6000. The sealed vessels were allowed to stay undisturbed for 4–6 days at 4 °C. Crystals of the orthorhombic as well as triclinic or monoclinic modifications appeared, frequently in the same droplet. Crystals were transferred to 5% PEG 10000 in the appropriate buffer conditions used for the microspectrophotometric analyses. No structure determination has yet been made on the CM-LADH–NADH complex in the closed conformation.

Results and Discussion

Low-Background Labeling of Cysteines Ensures Structural Integrity. Four to ten millimolar iodoacetate is frequently used to modify cysteine-46 of LADH. Enzyme reacted at these concentrations has been used in steady-state and transient kinetic experiments and for binding studies with coenzyme, substrates, and inhibitors (Reynolds & McKinley-McKee, 1975; Hardman, 1976; McFarland et al., 1977; Parker et al., 1978). This concentration range is about 100-fold higher than the concentration necessary to obtain total incorporation of the label on residue 46 (Zeppezauer et al., 1975). We observed that the enzyme samples labeled at the higher concentration of iodoacetate were unstable in solution, denatured rapidly, and could not be crystallized. Alkylation of cysteine-46 with 0.15 mM reagent yields a product which is stable as an NADH complex in solution for weeks, and the protein forms well-ordered crystals. This difference indicates that the enzyme maintains its structural integrity when the nonspecific background labeling of cysteine residues is low. Furthermore,

Table I: Accessible Surface Area (Å²) of the Sulfur Atoms of the 14 Cysteines per Subunit of Orthorhombic CM-LADH

residue	Å² units	remarks
Cys-9	0	localized in a groove on the surface of the molecule; surrounded by Thr, Tyr, main-chain atoms, and Lys-8 and -10
Cys-46	5	active-site zinc ligand; highest rate of alkylation[a] with haloacetates and related compounds; Arg-47 is situated at the entrance of the binding site and Arg-369 at the interior of the site
Cys-97	4	97–111 are ligands to the noncatalytic zinc binding site, comprised in a surface loop surrounded by Lys-99, -104,
Cys-100	0	-113, and -323 and Arg-101
Cys-103	4	
Cys-111	1	
Cys-132	0.5	localized at a shallow groove at the surface of the molecule with Arg-133 in front of the groove
Cys-170	0	situated in a cavity on the surface of the molecule; the Cys side chain is surrounded by Ala, Val, Ile, and Leu
Cys-174	0	active-site zinc ligand; preferentially reacts with iodoacetamide, coenzyme analogues,[b] diazonium-1*H*-tetrazole[c] and 3-bromopropionic acid[d]
Cys-195	0	buried in a hydrophobic environment
Cys-211	0	spatially a neighbor to Cys-195; further away from the surface of the molecule
Cys-240	0	situated at the bottom of a cavity on the surface of the molecule surrounded by Leu, Ala, and Lys
Cys-281	0	on the interior side of a surface loop covered by Arg-312
Cys-282	0	

[a] Reynolds & McKinley-McKee (1975), Dahl et al. (1976, 1979), and Dahl & McKinley-McKee (1977, 1981). [b] Jörnvall et al. (1975a,b). [c] Sogin & Plapp (1976). [d] Chadha & Plapp (1984).

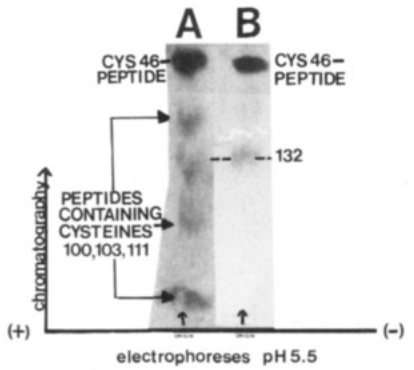

FIGURE 1: Distribution of radioactively labeled peptides of LADH-containing cysteines which are alkylated with iodo[2-^{14}C]acetate. (A) 10 mM reagent; (B) 0.15 mM reagent. At the position of the Cys-46 peptide, in the electrophoretogram, traces of the peptide containing Cys-97 might overlap. The remaining three peptides in sample A correspond to background labeling of cysteines ligated to the second metal binding site in the subunit (Figure 2).

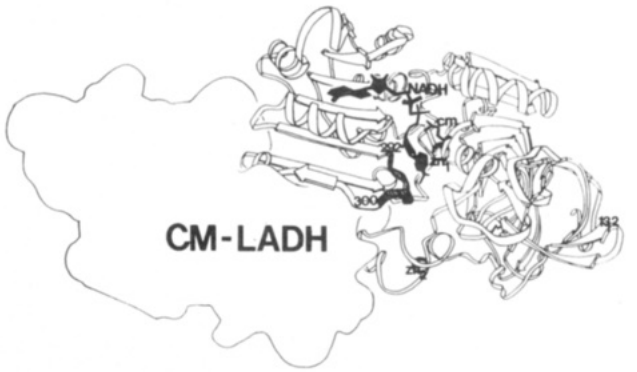

FIGURE 2: Schematic representation of dimeric LADH with one subunit outlined without secondary structure (drawing by Bo Furugren). The drawing illustrates the open conformation of LADH to which coenzyme is bound with the nicotinamide ring in the active site. CM denotes the carboxymethyl label on Cys-46, Zn_1 the catalytic zinc ion, and Zn_2 the noncatalytic zinc ion, which is ligated to four cysteine residues. The peptide loop 293–299, extending from strand βE, is marked in black. The location of residue 132 is indicated. This cysteine is weakly labeled, but no difference density in the Fourier maps could be observed in the three-dimensional structure determination.

crystalline CM-LADH–NADH complexes are formed which belong to the orthorhombic as well as to the triclinic or monoclinic modifications. The latter crystal forms are both characteristic for NADH complexes in which coenzyme binding has induced a large conformational change in the protein (Eklund et al., 1981, 1984; Samama, 1979; Schneider, 1983; Eklund & Brändén, 1983). This result shows that a catalytically competent crystal form (Bignetti et al., 1979) can be isolated in parallel with the NADH complex in the open structure of CM-LADH. Thus, specific carboxymethylation of Cys-46 does not prevent conformational transitions in the labeled protein.

Enzymic cleavage and analysis of the resulting peptide maps were performed in order to detect possible differences in the nonspecific background labeling of cysteines of the samples alkylated at high and low concentrations of iodoacetate. Sample A in Figure 1 (10 mM reagent) shows a pattern where four peptides are labeled in addition to the cysteine-46 peptide (Jörnvall, 1970a,b). The cysteines which are present in three of the extra peptides are cysteines-100, -103, and -111 [cf. Jörnvall & Pietrusko (1972) and Jörnvall (1973) for similar pictures]. Sample B of Figure 1 (0.15 mM reagent) shows background labeling only on one additional peptide (containing cysteine-132) which is common to both samples.

The LADH structure has two zinc atoms bound per subunit. One is ligated to cysteines-46 and -174 and histidine-67 and is the active-site zinc atom. The second zinc center is located 20 Å from the active site and is ligated to four cysteine residues (97, 100, 103, and 111). These cysteine residues are comprised in a polypeptide loop forming a small structural unit situated between the domains (Figure 2). The ligands to the second zinc ion apparently are susceptible to iodoacetate attack at 10 mM concentrations. This observation raises the following question: why are zinc-binding cysteines more susceptible to alkylation by iodoacetate than the eight free thiol groups in the subunit?

Accessibility calculations (Lee & Richards, 1971) of the orthorhombic (CM-LADH) structure show that the accessible surface area is about 5 Å² for the sulfurs of the zinc ligands 46, 97, and 103 and in the range 1–0 Å² for the zinc ligand 111 and Cys-132 located at the surface of the catalytic domain (Figure 2). For the remaining 9 of the 14 cysteine sulfurs (including the sulfur atom of cysteine-100 which is observed to be labeled), this area is 0 Å² (Table I). Thus, some of the cysteine sulfurs observed to be reactive are in fact accessible. In addition, arginine side chains are shown to be present in the vicinity of the reactive cysteines (Table I). The iodoacetate anion has been shown to bind reversibly prior to the attack of cysteine-46 (Reynolds & McKinley-McKee, 1969). Arginine-47 has been suggested to constitute part of the anion binding site (Zeppezauer et al., Brändén et al., 1975) during

this process. Arginine-133 might also assist in a reversible binding step in the reaction of cysteine-132. Furthermore, in the vicinity of the noncatalytic zinc, arginine-101 and lysine-99, -104, -113, and -323 may serve to anchor carboxylate groups of iodoacetate in a similar manner.

A structural role of the noncatalytic zinc center in LADH has been suggested earlier (Åkesson, 1964; Drum et al., 1967). Renaturation and refolding experiments have shown that zinc ions are needed for the refolding process of the protein (Rudolph et al., 1978). However, from these data, it was not possible to distinguish which of the two zinc binding sites in LADH was required first in order to fold the enzyme into the native structure. Our alkylation experiments provide strong experimental evidence that the noncatalytic zinc site adds to the structural stability of the protein. Buried and inaccessible cysteine residues (100 and 111) in the zinc binding loop became alkylated (Table I, Figure 1). This indicates that an alteration and an opening of the tight zinc binding structure seem to occur. In the presence of more than one alkyl group on the zinc ligands, it seems difficult to preserve the structural unit which the native noncatalytic zinc binding site represents. In addition, the zinc binding capacity of the site might be lost. In the enzyme preferentially labeled at Cys-46, the zinc content is unchanged compared to the native protein.

Microspectrophotometric Analyses. (*a*) *NADH Binding.* Single-crystal spectra were recorded on orthorhombic CM-LADH–NADH crystals, precipitated in MPD, in order to verify that the crystals of the open structure, used for the X-ray analysis, contained NADH. As a comparison, spectra were also recorded of crystals of the closed structure (LADH–NADH–dimethyl sulfoxide), precipitated with MPD (Eklund et al., 1981). NADH bound to CM-LADH, open conformation, has an absorption maximum at 330 nm, and NADH bound to the closed conformation has an absorption maximum at 320 nm. Similar results are obtained when spectra of the two crystalline CM-LADH–NADH complexes precipitated with PEG are compared (Figure 3A, open; 3B, closed). In Figure 3, spectra of various crystal complexes are compared. They represent typical measurements of a large number of samples. The 330-nm maximum thus can be distinguished from the two absorption maxima characteristic for NADH in a completely aqueous environment (340 nm) and NADH bound in the nonaqueous binding site of the closed structure of LADH (Eklund et al., 1984). It is evident from these results that the position of the absorption maximum for enzyme-bound NADH is correlated to the protein conformation and independent of the precipitating agents used.

(*b*) *Substrate Binding.* Crystals of the CM-LADH–NADH complexes (open and closed) were tested for their ability to convert substrates over the pH range 7–9.5; 20 mM benzaldehyde was added to orthorhombic crystals which were fully saturated with NADH. The decrease in the 330-nm absorption band was monitored in the single crystal. Complete oxidation of NADH was observed, but the crystals of this open complex slowly shattered.

The binding of the chromophoric substrate DACA to enzyme–coenzyme complexes is conveniently followed by means of microspectrophotometric measurements. A large shift of the absorption maximum of DACA is observed (Dunn & Hutchison, 1973) when the active-site metal–substrate bond is formed (Cedergren-Zeppezauer et al., 1982; Dunn et al., 1982). The magnitude of the shift depends on the oxidation state of the coenzyme (Dahl & Dunn, 1984a,b) as well as on the type of divalent ion present in the active-site metal center (Zeppezauer et al., 1984). Furthermore, studies with CM-

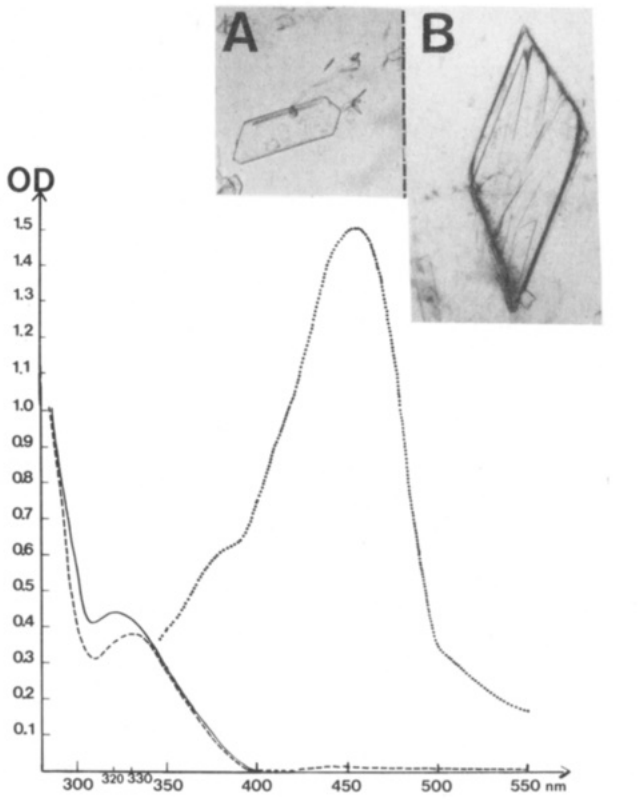

FIGURE 3: Light micrographs of the crystal forms obtained of Cys-46-carboxymethylated LADH–NADH complexes precipitated with PEG and single-crystal spectra recorded of four crystalline complexes. (A) Orthorhombic NADH complex precipitated in the presence of 1.5% PEG 10000 in the protein solution, at pH 7.8 in 0.05 M Tes/OH^-. (B) Triclinic or monoclinic crystals grown under similar conditions as in (A). (These crystal modifications of the closed form of LADH frequently grow together also in native samples.) (Solid line) Spectrum of triclinic or monoclinic crystals of the ternary complex with native LADH–NADH–dimethyl sulfoxide in MPD at pH 8.4 and 0.05 M Tris-HCl with a λ_{max} for protein-bound NADH at 320 nm. An identical spectrum is observed for triclinic or monoclinic CM-LADH–NADH crystals (B). 0.5 mM DACA (λ_{max} = 398 nm) solubilized in PEG at pH 7.8 was added to (B) crystals after the NADH spectrum had been recorded and the intense band with the λ_{max} at 456 nm rapidly developed (dotted line). (Dashed line) Spectrum of orthorhombic CM-LADH–NADH crystals precipitated either with PEG (A) or with MPD, pH 8.4, and 0.05 M Tris-HCl (the crystal type used for the X-ray analysis) with a λ_{max} for enzyme-bound NADH at 330 nm.

LADH have demonstrated that the spectral shifts for DACA, in complexes with NADH or NAD^+, are affected by the negative charge introduced on Cys-46 (Dahl & Dunn, 1984b).

A stable intermediate of zinc-bound DACA, at pH 9.5, in the presence of NADH could not be recorded, similar to what is observed for native crystalline complexes (Bignetti et al., 1979; Cedergren-Zeppezauer et al., 1982). However, addition of excess DACA to the CM-LADH–NADH in the closed structure, at pH 7.8, immediately gave an intense absorption band at 456 nm in the crystal (Figure 3). This value is nearly identical with that reported for the CM-LADH–NAD^+–DACA complex in solution (458 nm) (Dahl & Dunn, 1984b). It is thus apparent that a substrate conversion in the crystalline state has taken place. The crystals remain intact during NADH oxidation, and the abortive complex is stable at 10 °C. No external NADH is available around the crystals in the quartz cell; only a saturated solution of DACA (0.5 mM) is present. This permits a "single turnover" of substrates, and the abortive NAD^+–DACA complex can be trapped within the crystal [K_D(pH 7) = 10 μM for the CM-LADH–NAD^+(DACA) complex in solution] (Dahl & Dunn, 1984b).

The orthorhombic crystals of CM-LADH–NADH (Figure 3A) also formed an intense yellow complex with DACA at pH 7.8, but the reaction induced complete disintegration of the crystal lattice, and no spectra could be recorded. This is in contrast to the orthorhombic crystals of CM-LADH–NAD precipitated with MPD which were used for the X-ray analysis. We failed to detect any complex formation with DACA in these crystals over the pH range investigated. [The ternary triclinic LADH–NADH–DACA complex readily forms in the presence of 30% MPD (Bignetti et al., 1979).] One reason why DACA binding could not be observed in the orthorhombic crystals might be MPD binding in the substrate channel (see the following section). Our interpretation of the observation that crystals of the open complex with NADH were destroyed during substrate conversion is analogous to previous results obtained with crystalline substrate complexes (Cedergren-Zeppezauer et al., 1982; Eklund et al., 1982a). The structural changes which take place in the protein during catalysis cannot be accommodated in the orthorhombic lattice.

The microspectrophotometric analyses thus confirm that (1) NADH can bind to two protein conformations of CM-LADH and (2) the abortive NAD^+–aldehyde complex is formed in the closed structure. The spectra of the complex in the crystalline and solution states are similar, which indicates that the CM-LADH–NAD^+–DACA complexes have similar conformations in both states.

Three-Dimensional Structure of the CM-LADH–NADH (Open) Complex. The structure of the CM-LADH–NADH complex was determined to 3.2-Å resolution. The observed structure factors were combined with calculated phase angles from the refined native enzyme model determined to 2.4-Å resolution. One cycle of crystallographic refinement of the complex model, using the program CORELS, improved the R factor by 4% from 33% to 29%. Energy minimization in combination with crystallographic refinement, using the program EREF, further improved the model. The present interpretation of the interactions between NADH and Cys-46-carboxymethylated LADH is based on a model with an R factor of 26%. In a final structure factor calculation, 2707 atoms were included (97% of the total number of protein atoms, 2 zinc atoms, 1 coenzyme molecule, and the carboxymethyl group on Cys-46). Although the structure was solved to medium resolution, the difference Fourier maps were clear enough to interpret, except for two loop regions where the density for two or three amino acids was poorly defined. No difference electron density was visible for some of the surface side chains and a few interior amino acids (for instance, threonine-178 at the active site). No complete comparison with the native unliganded structure will be made at this resolution. Three outstanding features of the difference Fourier maps will be described in the present study: (1) The orientation of bound NADH; (2) the reorientation of the peptide loop 293–297; and (3) the distortion of the zinc ligand sphere.

(*a*) *NADH Interactions.* The electron density for the coenzyme extends from the adenine pocket to the active-site area, and the NADH model could be unambiguously fitted to the difference density (Figure 4A). The interactions between the protein and the AMP part of NADH in this complex are broadly similar to what has been described for coenzyme binding to both conformations of LADH (Eklund et al., 1981; Cedergren-Zeppezauer et al., 1982). It is apparent from earlier studies that the interactions between the protein and the nicotinamide mononucleotide (NMN) part of the coenzyme can differ widely in LADH complexes (Samama et al., 1977, 1981; Cedergren-Zeppezauer, 1983).

NADH binding to orthorhombic CM-LADH occurs without induction of the rotations of domains. Calculations based on a comparison of the α-carbon atoms of the separate domains (excluding one loop region) of the CM-LADH structure and native, unliganded LADH show that the structures are similar within the error limit for the structure determination. Nevertheless, the nicotinamide ring is localized within the active site close to the position found for triclinic coenzyme complexes (Figure 4B). This similarity is of particular interest since a structural change of the peptide loop 293–297 has taken place, compared to the native open structure (see below), and corresponds to a similar peptide movement in the triclinic complex. In addition, the position of the adenosine part of NADH is shifted about 1 Å compared to coenzymes bound to orthorhombic complexes in which a loop movement is absent (Cedergren-Zeppezauer et al., 1982; Cedergren-Zeppezauer, 1983). In a recent report by Eklund et al. (1984), coenzyme interactions with LADH are described in great detail as well as the domain movements in the subunit induced by coenzyme binding. We will refer to data listed in this report in the following comparison. The superposition of the structures is based on calculations in which the transformation matrix for the triclinic coordinate set is derived from the equivalence between α-carbon atom positions in the β-sheet structure of the coenzyme binding domain (Ohlsson et al., 1974).

A comparison of the coordinates for the coenzyme models shows that the positions of the nicotinamide ring and nicotinamide ribose differ in the distance range 0.4–0.7 Å. The tilt of the nicotinamide ring is similar within $\sim 10°$. The largest differences are observed for atoms in the pyrophosphate bridge (1.2–3 Å). The change in the position of the adenosine part of NADH is roughly 1 Å. This is due to the rather complex conformational change in the protein [cf. Eklund et al. (1984) for a comparison between ADP-ribose and NADH] and thus not solely the effect of the loop motion mentioned above.

The interactions between the nicotinamide ring and active-site residues differ in the two structures. The ring is not located as close to the zinc atom and its ligands in the CM-LADH complex as observed for triclinic complexes. The labeled SG 46 is 6 Å from the C5N and C6N atoms. Instead, one oxygen atom of the carboxymethyl group seems to make the van der Waals contact to this part of the ring. The differences observed in the zinc positions in Figure 5 are the influence of the rotation of the catalytic domain in the triclinic structure.

On the B side of the nicotinamide plane, the interactions in the two structures are very similar (Figures 4B and 5). In addition to valine-203 (not shown), the side chains of valine-292 and -294 form hydrophobic contacts. The carbonyl oxygen of residue 292 points to the C2N atom of the ring at a distance of 3.2 Å. Threonine-178 (tentatively fitted in this structure) interacts from the B-side direction. Thus, three oxygen atoms are close to the nicotinamide ring in CM-LADH.

The carboxamide group is coplanar to the pyridine ring in our present model of NADH. This gives a satisfactory fit to the difference density (Figure 4A) at this resolution. Suitable distances and favorable angles for hydrogen-bond interactions are found between N2N–O=C292 and O1N–N319. A rotation of the carboxamide group out of the plane by 30°, similar to that proposed for NADH bound to triclinic LADH, would impair these interactions. The hydrophobic interactions to residues 317–319 as well as the hydrogen bond to the

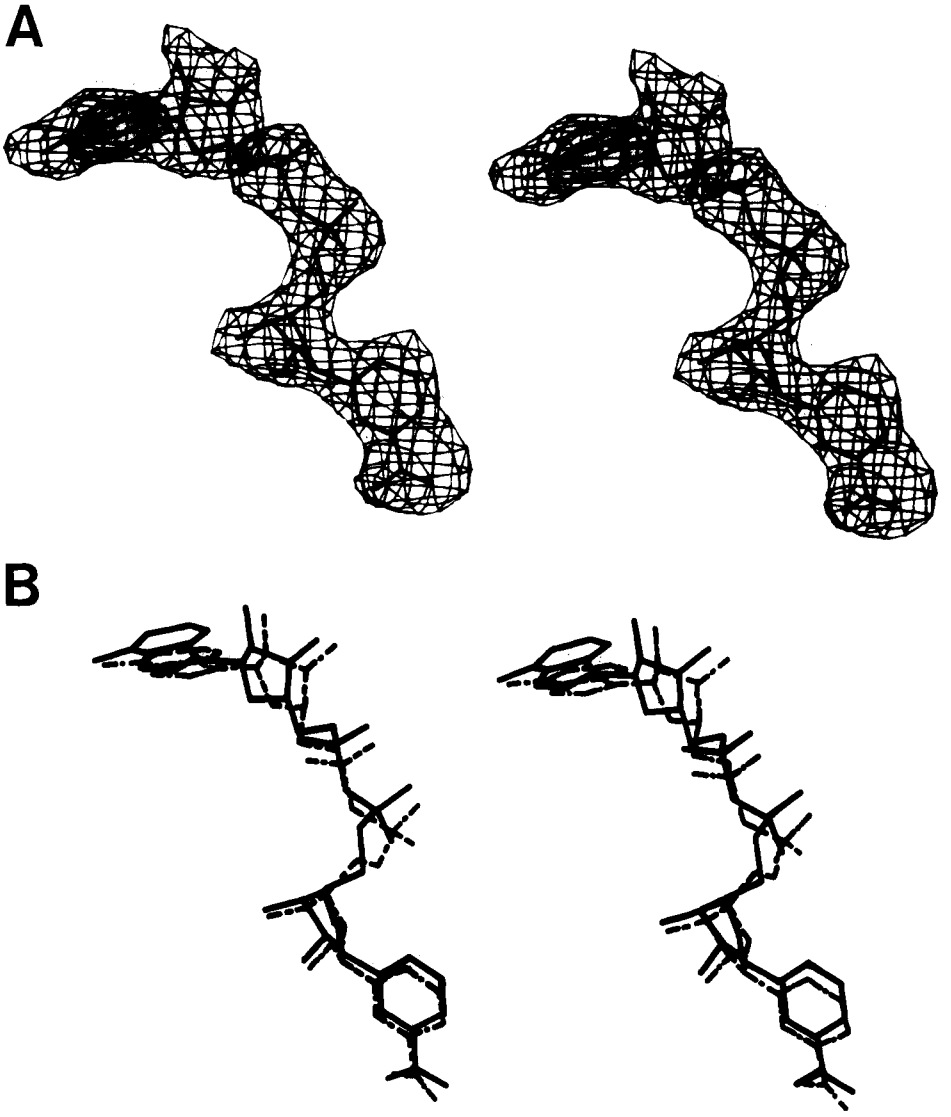

FIGURE 4: (A) Difference electron density of NADH (bound to CM-LADH) from the $F_{obsd} - F_{calcd}$ Fourier map. The coordinates for the coenzyme model were subtracted in the structure factor calculation. (B) Stereo diagram of the NADH model derived from this map (solid lines) compared to NADH bound to triclinic native LADH (dashed lines).

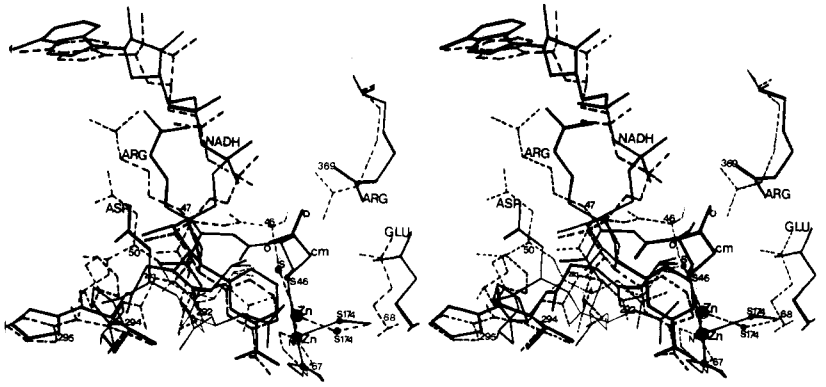

FIGURE 5: Stereo diagram which compares part of the active site of the Cys-46-carboxymethylated LADH–NADH complex (solid lines) with the native LADH–NADH–dimethyl sulfoxide complex (dashed lines). For clarity, the zinc-bound inhibitor is not shown in the picture. The coordinates for the triclinic structure are those deposited at the Protein Data Bank (Eklund et al., 1984). The diagram illustrates the differences in the orientations of Arg-47 and -369 coupled to the acidic groups Asp-50 and Glu-68 in relationship to the pyrophosphate bridge of NADH.

carbonyl oxygen of residue 317 observed in the triclinic complex are missing.

In the triclinic structure, two arginine side chains, 47 and 369, contribute in compensating for the negative charges on the pyrophosphate group. Both are coupled to acidic groups, Arg-47–Asp-50–Arg-363 and Arg-369–Glu-68. The rigid-body rotation of the catalytic domain moves the Arg-47–Asp-50 ion pair toward the coenzyme binding cleft. The slight rotation of the coenzyme domain moves the coenzyme toward the Arg-369–Glu-68 couple located at the interior of the binding site (Eklund et al., 1984). Since no domain movements occur in the orthorhomic structure, no direct interaction be-

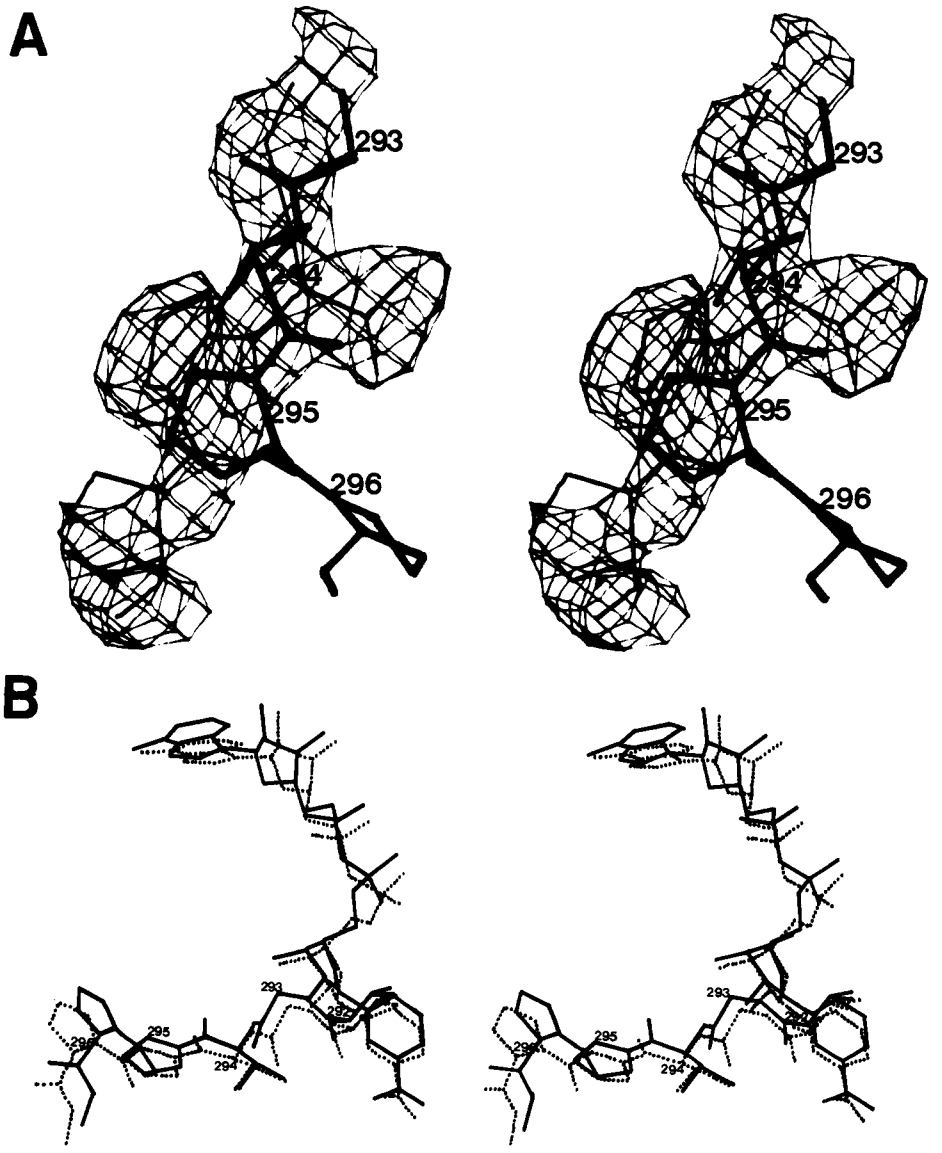

FIGURE 6: (A) Part of the $2F_{obsd} - F_{calcd}$ Fourier map showing the fitting of the model of the loop region 293–296 in the CM-LADH complex. Thick lines show the superposition of the same residues of native LADH. (B) Comparison of the loop with triclinic LADH.

tween Arg-369 and the pyrophosphate bridge is established in the CM-LADH complex. The carboxymethyl label of Cys-46 occupies the space between these groups. Compared to native unliganded LADH, the side chain of Arg-369 is slightly moved, but the contact to Glu-68 is not broken in CM-LADH. Instead, a CM-Arg-Glu triad has been formed. The side chain of Arg-47 is clearly observed in the Fourier maps, and the guanidinium group is 3.5 Å from the pyrophosphate bridge. However, the Arg-47–Asp-50 ion pair has been separated. The distances are 5 Å between members in the Arg-47–Asp-50–Arg-363 triad in the CM-LADH structure. Figure 5 illustrates the differences in the interactions around the pyrophosphate bridge in the two structures.

Neither His-51 and Ser-48 nor Lys-228 forms hydrogen bonds to the ribose rings of NADH. In summary, the domain movements, which create the major differences between orthorhomic CM-LADH and triclinic LADH, affect the NADH interactions such that six additional hydrogen bonds and several van der Waals contacts are formed in the triclinic complex. The accessible surface area for NADH is thereby reduced by 6%. The comparison of the accessible surface areas was made from calculations in which a fourth, non-protein ligand to zinc had been excluded.

The partial shielding of the nicotinamide ring in the open CM-LADH complex offers a satisfactory structural explanation for the smaller blue shift of the NADH spectrum (Figure 3).

(*b*) *Structural Change in the Peptide Loop 293–299.* The loop 293–299 is the continuation of strand βE in the six-membered β-sheet structure of the coenzyme binding domain [for nomenclature of secondary structure elements, see Eklund et al. (1976)] and has the sequence Gly-Val-Pro-Pro-Asp-Ser-Glu (Jörnvall, 1970a). The amino end of the loop is situated within the hydrophobic active-site area and contributes to the formation of the nicotinamide binding site. The last three amino acids are exposed on the surface of the subunit. Beyond residue 300, the polypeptide chain again forms a defined secondary structure comprising the subunit–subunit interaction surface (Figure 2).

It is clearly observed in the orthorhombic CM-LADH structure that a structural change takes place in the loop, when NADH is bound, compared to orthorhombic apoenzyme. From the difference density maps, calculated without the contribution of the atoms or residues 292–300 to the structure factors, it was obvious how to trace the main chain for these residues. However, the density for some atoms of the surface

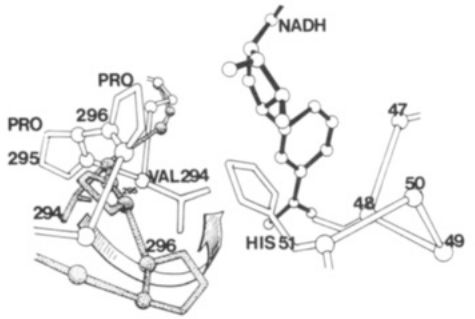

FIGURE 7: Schematic representation of part of the domain–domain contact area of the subunit in the vicinity of the active site of LADH. (Open lines) The polypeptide backbone in the orthorhombic CM-LADH–NADH complex with part of the coenzyme model in black. (Dotted model) Part of the loop 292–296 in apo-LADH. The arrow indicates that residue 294, buried in the apoenzyme, enters the coenzyme binding region in the CM-LADH structure. Thereby, the entrance into the nicotinamide binding sites becomes blocked from one direction.

residues Asp and Ser is poor, and the orientation of these side chains is tentative. Figure 6A shows the fit of residues Gly-Val-Pro-Pro to the difference density map with the model of the same side chains of the native unliganded enzyme superimposed. The chains have different directions in this part of the loop but overlap perfectly again at position Glu-299, for which the density is good (Figure 7). It is important to note that the orientation of the loop residues is similar in the CM-LADH–NADH structure compared to the closed conformation (Figure 6B).

(*c*) *Active-Site Zinc Environment.* The catalytic zinc atom is ligated to cysteines-46 and -174, histidine-67, and a water molecule in the apoenzyme (Eklund et al., 1976). In the orthorhombic CM-LADH–NADH complex, the zinc coordination sphere is highly distorted. The carboxymethyl group on cysteine-46 could be identified in the difference Fourier maps as an extension from the cysteine side chain (Figure 8). The presence of NADH plus the charged label in the ac-

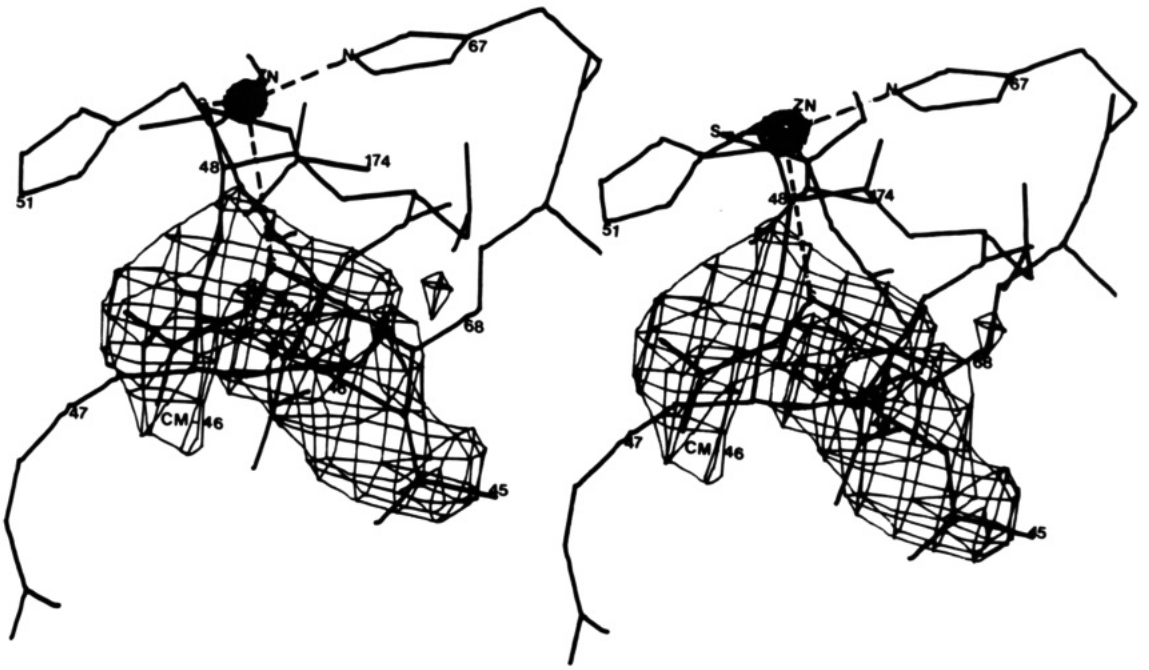

FIGURE 8: Region around carboxymethylated cysteine-46 showing the difference density for the label plotted from a Fourier map in which the contributions of all residues in the metal binding sphere have been omitted in the structure factor calculation. The residues 45–51, 67, and 68 in addition to cysteine-174 are displayed.

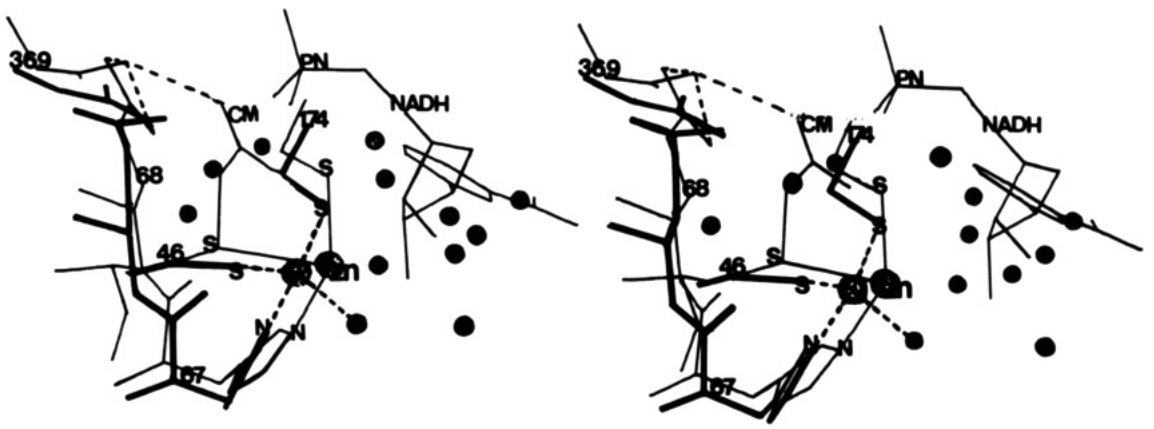

FIGURE 9: Stereo diagram which compares the active-site zinc sphere of the Cys-46-carboxymethylated LADH–NADH complex (thin lines) with native unliganded enzyme (thick lines). The coordinates for the native structure are those deposited at the Protein Data Bank. Dashed lines connect the ligands to zinc in native LADH which has a tetrahedral geometry. Dashed lines in the CM-LADH structure indicate the position of the carboxylate group of the label (CM) at a hydrogen-bond distance to Arg-369, which in turn is hydrogen bonded to Glu-68. The CM group is at van der Waals distance to the OP1N atom of NADH. Black dots denote bound water molecules in the unliganded native enzyme, most of which are displaced in the complex.

tive-site area influences the positions of many amino acids in the immediate surrounding of the zinc coordination sphere, as well as the zinc ion position. The center of the peak for the metal atom is shifted by 1 Å compared to the position of the zinc atom in the unliganded enzyme. The movement is in the direction toward the substrate binding site. The distance between the sulfur of residue 46 and the metal in the CM-LADH complex has been interpreted to be of the order of 3 Å compared to 2.3 Å in native LADH in both conformations. The difference density maps do not show a peak at the fourth ligand position to the metal (occupied by substrate or inhibitor in other coenzyme complexes). This cannot be taken as evidence that the fourth ligand position in this complex is not occupied. It might rather indicate an effect of the limited resolution of the structure determination. Therefore, a detailed description of the geometry of the metal coordination sphere cannot be made on the basis of our present results. In the comparison made in Figure 9, it is apparent that most of the water molecules, bound in the neighborhood of the zinc coordination sphere in native apo-LADH, become exchanged either by the coenzyme or by the carboxymethyl group in CM-LADH.

Elongated densities are observed in the substrate channel, 6 Å from zinc and linked at a distance of 3 Å to the N2N atom of the carboxamide group of NADH. The totally hydrophobic region in the channel, further away from the zinc atom, is also occupied. In previous studies of LADH, we have interpreted densities located in the substrate channel as MPD binding. It is highly probable that MPD also binds in this CM-LADH complex and interferes with DACA binding. The microspectrophotometric measurements of the orthorhombic CM-LADH–NADH crystals (MPD precipitation) clearly demonstrated that DACA had no access to the zinc center which is situated deepest in the 15-Å-long channel.

ACKNOWLEDGMENTS

We express our gratitude to Professor Hans Jörnvall and Dr. Hedvig von Bahr, Karolinska Institute, Stockholm, for their assistance in the peptide analysis work and for critical reading of the manuscript. A travel grant from the Swedish Natural Science Research Council and the generosity of Professor Gian-Luigi Rossi enabled E.S.C.-Z. to perform microspectrophotometric measurements at the University of Parma, Italy, which is gratefully acknowledged. We thank Professors C.-I. Brändén and M. Zeppezauer for valuable discussions during the course of the work and M. F. Dunn for communication of data prior to publication. Thanks are due to Dr. A. T. Jones for access to phase angles during the refinement of native LADH, to Dr. Eklund for preparing the calculation with the program COREL, and to Eduardo Horjales for advice concerning the program EREF. Furthermore, we thank Anita Rogelius and Irmgard Kurland for help in preparing the manuscript and for language revision.

Registry No. DACA, 20432-35-3; Cys, 52-90-4; S, 7704-34-9; Zn, 7440-66-6.

REFERENCES

Bignetti, E., Rossi, G. L., & Zeppezauer, E. (1979) *FEBS Lett. 100*, 17–22.

Brändén, C.-I., Jörnvall, H., Eklund, H., & Furugren, B. (1975) *Enzymes, 3rd Ed. 11*, 103–190.

Carlsson, L., Nyström, L.-E., Lindberg, U., Kannan, K. K., Cid-Dresner, H., Lövgren, S., & Jörnvall, H. (1976) *J. Mol. Biol. 105*, 353–366.

Cedergren-Zeppezauer, E. (1983) *Biochemistry 22*, 5761–5772.

Cedergren-Zeppezauer, E., Samama, J.-P., & Eklund, H. (1982) *Biochemistry 21*, 4895–4908.

Chadha, V. K., & Plapp, B. V. (1984) *Biochemistry 23*, 216–221.

Dahl, K. H., & McKinley-McKee, J. S. (1977) *Eur. J. Biochem. 81*, 223–235.

Dahl, K. H., & McKinley-McKee, J. S. (1981) *Eur. J. Biochem. 118*, 507–513.

Dahl, K. H., & Dunn, M. F. (1984a) *Biochemistry 23*, 4094–4100.

Dahl, K. H., & Dunn, M. F. (1984b) *Biochemistry 23*, 6829–6839.

Dahl, K. H., McKinley-McKee, J. S., & Jörnvall, H. (1976) *FEBS Lett. 71*, 287–290.

Dahl, K. H., McKinley-McKee, J. S., Beyerman, C. H., & Noorman, A. (1979) *FEBS Lett. 99*, 308–312.

Dalziel, K. (1963) *J. Biol. Chem. 238*, 2850–2858.

Drum, D. E., Harrison, J. H., Li, T.-K., Bethune, J. L., & Vallee, B. L. (1967) *Proc. Natl. Acad. Sci. U.S.A. 57*, 1434–1440.

Dunn, M. F., & Hutchison, J. S. (1973) *Biochemistry 12*, 4882–4892.

Dunn, M. F., Dietrich, H., MacGibbon, A. K. H., Koerber, S. C., & Zeppezauer, M. (1982) *Biochemistry 21*, 354–363.

Eklund, H., & Brändén, C.-I. (1979) *J. Biol. Chem. 254*, 3458–3461.

Eklund, H., & Brändén, C.-I. (1983) in *Zinc Enzymes* (Spiro, T., Ed.) Wiley, New York.

Eklund, H., Nordström, B., Zeppezauer, E., Söderlund, G., Ohlsson, I., Boiwe, T., Söderberg, B.-O., Tapia, O., Brändén, C.-I., & Åkeson, Å. (1976) *J. Mol. Biol. 102*, 27–59.

Eklund, H., Samama, J. P., Wallén, L., Brändén, C.-I., Åkeson, Å., & Jones, T. A. (1981) *J. Mol. Biol. 146*, 561–587.

Eklund, H., Plapp, B. V., Samama, J.-P., & Brändén, C.-I. (1982a) *J. Biol. Chem. 257*, 14349–14358.

Eklund, H., Samama, J. P., & Wallén, L. (1982b) *Biochemistry 21*, 4858–4866.

Eklund, H., Samama, J.-P., & Jones, T. A. (1984) *Biochemistry 23*, 5982–5996.

Evans, N., & Rabin, B. R. (1968) *Eur. J. Biochem. 4*, 548–554.

Hardman, M. J. (1976) *Eur. J. Biochem. 66*, 401–406.

Jack, A., & Levitt, M. (1978) *Acta Crystallogr., Sect. A: Cryst. Phys., Diffr., Theor. Gen. Crystallogr. A34*, 931–935.

Jones, D. T., & Khalifah, R. G. (1980) *Adv. Exp. Med. Biol. 132*, 77–83.

Jones, T. A. (1982) in *Computational Crystallography* (Sayre, D., Ed.) pp 303–317, Oxford University Press, New York.

Jörnvall, H. (1970a) *Eur. J. Biochem. 16*, 25–40.

Jörnvall, H. (1970b) *Eur. J. Biochem. 16*, 41–49.

Jörnvall, H. (1973) *Biochem. Biophys. Res. Commun. 53*, 1096–1101.

Jörnvall, H., & Pietruszko, R. (1972) *Eur. J. Biochem. 25*, 283–290.

Jörnvall, H., Woenckhaus, C., & Jonscher, G. (1975a) *Eur. J. Biochem. 53*, 71–81.

Jörnvall, H., Woenckhaus, C., Schättle, E., & Jeck, R. (1975b) *FEBS Lett. 54*, 297–301.

Kamlay, M. T., & Shore, J. D. (1983) *Arch. Biochem. Biophys. 222*, 59–66.

Khalifah, R. G., & Sutherland, W. M. (1979) *Biochemistry 18*, 391–398.
Lee, B., & Richards, F. M. (1981) *J. Mol. Biol. 55*, 379–400.
McFarland, J. T., Chen, J., Wnuk, M., DeTraglia, M. C., Li, T. Y., Petersen, R., Jacobs, J. W., Schmidt, J., Feinberg, B., & Watters, K. L. (1977) *J. Mol. Biol. 115*, 365–380.
Morris, R. G., Saliman, G., & Dunn, M. F. (1980) *Biochemistry 19*, 725–731.
Ohlsson, I., Nordström, B., & Brändén, C.-I. (1974) *J. Mol. Biol. 89*, 339–354.
Parker, D. M., Hardman, M. J., Plapp, B. V., Holbrook, J. J., & Shore, J. D. (1978) *Biochem. J. 173*, 269–275.
Reynolds, C. H., & McKinley-McKee, J. S. (1970) *Eur. J. Biochem. 14*, 14–26.
Reynolds, C. H., & McKinley-McKee, J. S. (1975) *Arch. Biochem. Biophys. 168*, 145–162.
Reynolds, C. H., Morris, D. L., & McKinley-McKee, J. S. (1969) *Eur. J. Biochem. 10*, 474–478.
Rudolph, R., Gerschitz, J., & Jaenicke, R. (1978) *Eur. J. Biochem. 87*, 601–606.
Samama, J. P. (1979) Ph.D. Thesis, l'Université Louis Pasteur de Strasbourg, Strasbourg, France.
Samama, J. P., Zeppezauer, E., Biellmann, J.-F., & Brändén, C.-I. (1977) *Eur. J. Biochem. 81*, 403–409.
Samama, J. P., Wrixon, A. D., & Biellmann, J. F. (1981) *Eur. J. Biochem. 118*, 479–486.
Schneider, G. (1983) Ph.D. Thesis, University of Saarbrücken, FRG.
Schneider, G., Eklund, H., Cedergren-Zeppezauer, E., & Zeppezauer, M. (1983) *EMBO J. 2*, 685–689.
Shore, J. D., & Gutfreund, H. (1970) *Biochemistry 9*, 4655–4659.
Sogin, D. C., & Plapp, B. V. (1976) *Biochemistry 15*, 1087–1093.
Sussmann, J. L., Holbrook, S. R., Church, G. M., & Kim, S.-H. (1977) *Acta Crystallogr., Sect. A: Cryst. Phys., Diffr., Theor. Gen. Crystallogr. A33*, 800–804.
Syvertsen, C., & McKinley-McKee, J. S. (1983) *Arch. Biochem. Biophys. 223*, 213–223.
Taniguchi, S., Theorell, H., & Åkeson, Å. (1967) *Acta Chem. Scand. 21*, 1903–1920.
Theorell, H., & McKinley-McKee, J. S. (1961) *Acta Chem. Scand. 15*, 1811–1833.
Zeppezauer, E., Jörnvall, H., & Ohlsson, I. (1975) *Eur. J. Biochem. 58*, 95–104.
Zeppezauer, M., Andersson, I., Dietrich, H., Gerber, M., Maret, W., Schneider, G., & Schneider-Bernlöhr, H. (1984) *J. Mol. Catal. 23*, 377–387.

Rate-Limiting Steps in the DNA Polymerase I Reaction Pathway†

V. Mizrahi, R. N. Henrie, J. F. Marlier, K. A. Johnson, and S. J. Benkovic*
Departments of Chemistry and Biochemistry, The Pennsylvania State University, University Park, Pennsylvania 16802
Received September 27, 1984

ABSTRACT: The initial rates of incorporation of dTTP and thymidine 5′-*O*-(3-thiotriphosphate) (dTTPαS) into poly(dA)·oligo(dT) during template-directed synthesis by the large fragment of DNA polymerase I have been measured by using a rapid-quench technique. The rates were initially equal, indicating a non-rate-limiting chemical step. However, the rate of thionucleotide incorporation steadily diminished to 10% of its initial value as the number of consecutive dTMPαS residues in the primer strand increased. This anomalous behavior can be attributed to the helix instability inherent in phosphorothioate-containing duplexes. Positional isotope exchange experiments employing the labeled substrate [α-$^{18}O_2$]dATP have revealed negligible α,β-bridging → β-nonbridging isotope exchange in template-directed reactions of *Escherichia coli* DNA polymerase I (Pol I) both in the presence and in the absence of added inorganic pyrophosphate (PP_i), suggesting rapid PP_i release following the chemical step. These observations are consistent with a rate-limiting step that is tentatively assigned to a conformational change of the E·DNA·dNTP complex immediately preceding the chemical step. In addition, the substrate analogue (S_P)-dATPαS has been employed to examine the mechanism of the PP_i exchange reaction catalyzed by Pol I. The net retention of configuration at the α-P is interpreted in terms of two consecutive inversion reactions, namely, 3′-hydroxyl attack, followed by PP_i attack on the newly formed primer terminus. Kinetic analysis has revealed that while α-phosphorothioate substitution has no effect upon the initial rate of polymerization, it does attenuate the PP_i exchange reaction by a factor of 15–18-fold. The mechanistic implications of these results are discussed.

Escherichia coli DNA polymerase I (Pol I)[1] is a relatively well-characterized multifunctional enzyme involved in the repair and replication of DNA in vivo. In addition to the polymerase capacity, which catalyzes the incorporation of mononucleotide residues derived from deoxyribonucleoside 5′-triphosphates (dNTPs) into the 3′ end of an appropriate template-primer, the enzyme is also capable of catalyzing DNA degradation by means of distinct 3′→5′- and 5′→3′-

† This research was supported by Grants GM13306 (to S.J.B.) and GM26726 (to K.A.J.) from the National Institutes of Health.
* Address correspondence to this author at the Department of Chemistry, The Pennsylvania State University.

[1] Abbreviations: Pol I, *Escherichia coli* DNA polymerase I; KF, Klenow fragment; PP_i, inorganic pyrophosphate; (●), ^{18}O; kDa, kilodalton(s); PEP, phosphoenolpyruvate; TLC, thin-layer chromatography; HPLC, high-pressure liquid chromatography; PIX, positional isotope exchange; TEAB, triethylammonium bicarbonate; Tris·HCl, tris(hydroxymethyl)aminomethane hydrochloride; GC–MS, gas chromatography–mass spectroscopy; b, bridging; nb, nonbridging; EDTA, ethylenediaminetetraacetic acid; dTTPαS, thymidine 5′-*O*-(3-thiotriphosphate); dTMPS, 2′-thymidine 5′-*O*-phosphorothioate.

0006-2960/85/0424-4010$01.50/0